# Electronic conductivity in GDC under DC bias as a trigger for flash sintering

Tarini Prasad Mishra[1,2,#], Rubens Roberto Ingraci Neto[2], Giorgio Speranza[3], Alberto Quaranta[4] , Vincenzo M. Sgalvo[4] , Rishi Raj[2], Olivier Guillon[1,5], Martin Bram[1], Mattia Biesuz[4,#]

[1] Institute of Energy and Climate Research: Materials Synthesis and Processing (IEK-1), Forschungszentrum Jülich GmbH, Jülich 52425, Germany

[2] Materials Science and Engineering Program, Department of Mechanical Engineering, University of Colorado Boulder, Boulder, Colorado

[3] Fondazione Bruno Kessler, Via Sommarive 18, Trento 38123, Italy

[4] Department of Industrial Engineering, University of Trento, Via Sommarive 9, Trento 38123, Italy

[5] Jülich Aachen Research Alliance, JARA-Energy, Germany

[#] **Corresponding authors:** T.M. t.mishra@fz-juelich.de

M.B. mattia.biesuz@unitn.it

**Abstract**

In this paper, we discuss the progression of flash sintering in 10 mol% gadolinium-doped ceria specimens (GDC10). The flash transition is correlated with the generation of *n-type* electronic conductivity in ambient air under DC bias. Its origin is attributed to a partial reduction of the material which propagates from the cathodic to the anodic region, during the incubation period. The phenomenon was observed, *in-situ*, by monitoring the development of electrochemical blackening during the incubation period of the flash experiment. Anomalous features, including a shift in the valence band edge, shrinkage of the band gap and a change in the oxidation state of Ce in flashed samples was confirmed by XPS and diffuse reflectance measurements. The results prove that flash sintering can alter the electronic structure of GDC10, such alterations being partially retained after the flash.

**Main body**

Flash sintering (FS) is a novel field/current-assisted sintering techniques for rapidly densifying ceramics at low furnace temperatures [1-5]. It is usually described by three stages. First, a constant electric field is applied to the green body while it is heated inside a furnace (*Stage I*). Then, the flash event is signaled by a non-linear rise in the sample conductivity at a critical furnace temperature (*Stage II*). Here, the electric power source switches from voltage to current control (because of the huge increase in the electrical conductivity of the ceramic) and the sample densifies in a few seconds while emitting a bright glow. The flash event takes place at specific power dissipation value regardless the external furnace temperature in the 300-1300°C range [6]. Finally, a steady state condition is reached in current control (*Stage III*). The features of FS can be summarized as: (i) non-linear rise in conductivity [1], (ii) photoemission [7-8] and (iii) rapid densification [9-11]. Moreover, the Debye temperature is currently emerging as a lower bound for the flash onset [12-14]. Nevertheless, the underlying mechanisms of flash sintering remain controversial [15-22].

Gadolinium-doped ceria (GDC) is a $O^{2-}$ ion conductor with applications in energy conversion devices such as Solid Oxide Fuel Cell (SOFC) and Solid Oxide Electrolyzer Cell (SOEC). FS of GDC has been extensively studied [23-25] with a specific focus on the densification process. An important insight was presented by Jha et al. [26], who measured abnormal lattice expansion by *in-situ* X-ray diffraction during FS. Here, we address the influence of flash processing on the change in chemical and physical properties such as electrical conductivity.

Recently, Zhang & Luo [27] showed that the onset flash temperature of ZnO is lowered in reducing atmosphere (Ar/5%$H_2$) down to 120°C . Although this behavior was quite expected in *n-type* electronic semiconductors (i.e., in ZnO), it would be more unusual in an oxygen ion conductor where the charge carrier concentration,$V_O^{\cdot\cdot}$, is given by the substitution element (i.e., the gadolinium GDC). However, recent works on yttria-stabilized zirconia (YSZ) suggested that the flash can introduces additional charge transport mechanisms [28-29]; in particular, Jo and Raj proved the activation of electronic conductivity in YSZ by *in-situ* electrochemical impedance spectroscopy [30]. Electronic conductivity is expected to be strongly dependent on the oxygen partial pressure in the atmosphere; thus, here we question whether electronic conductivity could be activated also in GDC and change its flash onset temperature. In summary, we seek a deeper understanding of the origin of flash transition for GDC10. This goal is achieved by exploring the electrochemical effects and the related enhancement in electronic conductivity under DC field.

Commercial gadolinium-doped ceria ($Gd_{0.10}Ce_{0.90}O_{1.95}$: GDC10, Fuelcellmaterials, USA) powder was used in this work. The average particle size, $d_{50}$ = 0.13 µm, and the specific surface area, 10.5 m $g^{-1}$, were measured with a particle size analyzer Horiba LA-950 V2 (Retsch Technology GmbH, Haan, Germany) and Area Meter II (Ströhlein Instruments, Viersen, Germany), respectively.

Dog bone-like samples were prepared by uniaxial pressing at 100 MPa for constant heating rate flash sintering experiments in air and Ar/5%$H_2$. The samples had a gauge-length of 15 mm and cross-section 3.3 x 1.9 $mm^2$. The green bodies were too fragile and difficult to connect to the electrodes. To overcome these challenges, the samples were pre-sintered at 1000°C for 30 minutes (heating and cooling rate = 3 K $min^{-1}$). The relative densities of the green body and of the pre-sintered samples, were approximately 55% and 62% of the theoretical one.

To perform FS experiments the samples were connected to the power source by mean of platinum wires, which served as electrodes. Platinum paste was spread at the metal/ceramic interface to ensure good electrical contact. The experiments were carried out in a tubular furnace (experimental

set-up reported in [31]) at a constant rate of 10 K $min^{-1}$. Two different atmospheres were used: lab air and Ar/5% $H_2$. The electric fields were applied by using a Sorensent DLM300-2 power source (AMETEK Programmable Power, Inc., San Diego, CA); the current limit was set at 100 mA $mm^{-2}$. The current flowing through the sample and the voltage were measured with a digital multimeter (Keithley 2000, Keithley Instruments, Cleveland, USA). After the flash event, the specimens were held at the current limit for 30 s.

Additional dog-bone samples were produced to check possible electrochemical effects upon FS. Their gage length and cross section were 20 mm and 3.0 x 2.0 $mm^2$, respectively. The samples were sintered at 1250°C for 2 h (heating rate of 10 K $min^{-1}$) in static air (density ~90%). The flash experiment was carried out in air on a hot plate at about 280°C (isothermal FS). Pt wires served as electrodes and were connected to a DC power supply (Sorensen DLM 300-2). To improve the ceramic-metal contact Pt paste was spread at the interface. An electric field of 175 V $cm^{-1}$ was used to activate the flash and the current limit was fixed at 25 mA $mm^{-2}$. Electric data were monitored using a Keitheley 2100 multimeter (Keithley Instruments, Cleveland, USA) and a video of the experiment was taken using a digital camera with the aim to check the presence of electrochemical blackening. After the flash, the sample was characterized by XRD, XPS and diffuse reflectance spectroscopy. XRD was carried out in an Italstructures IPD3000 diffractometer (Co Kα X-rays source) equipped with an Inel CPS120 detector. XPS was performed with an Axis DLD Ultra spectrometer (Kratos – Manchester UK) with an energy step of 0.05 eV. The spectra were aligned on the binding energy scale taking the C 1s at 285 eV as a reference. The different components of the XPS spectra were assigned according to the literature [32-33]. Diffuse reflectance spectra were collected by using an Ocean Optics QE65000 spectrometer and a halogen lamp light source (Top sensor systems, DH-2000-S). The calibration was carried out using a MgO standard (Sigma Aldrich). The bandgap energy was estimated by drawing the tangent at the inflection point of the $(F_{(R)}E)^2$ function vs. photon energy (E) plot, $F_{(R)}$ being the Kubelka-Munk function [34]:

$$F_{(R)} = \frac{(1-R)^2}{2R} \qquad \text{Eq. 1}$$

where R is the diffuse reflectance.

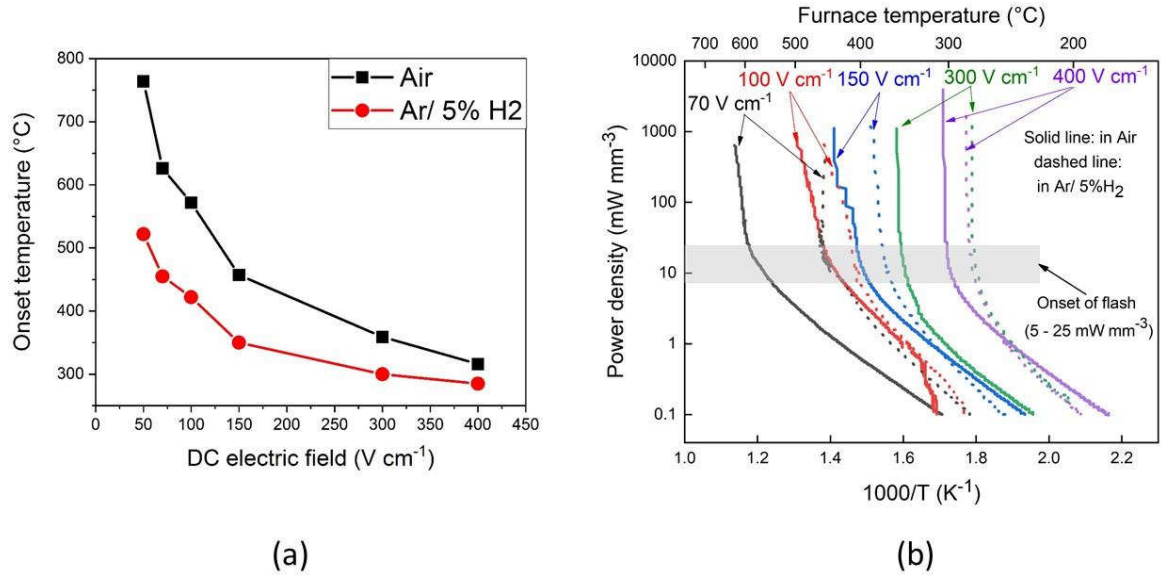


(a) (b)

Figure 1. (a) Onset temperature for FS in pre-sintered GDC10 specimen as a function of the electric field in air and Ar/5%$H_2$ (heating rate = 10 K $min^{-1}$); (b) Arrhenius plots

of power density for GDC10 pre-sintered specimen in air and Ar/5%$H_2$ showing the transition to non-linear rise in conductivity. Experiments were carried out at a heating rate 10°C/min and the maximum current density was set to 100 mA $mm^{-2}$. "T" in (b) represents the furnace temperature.

The onset flash temperature for pre-sintered GDC10 samples (relative density ≈ 61%) decreases in reducing atmosphere, i.e. Ar/$H_2$ (Figure 1 (a)). The effect is pronounced at moderate values of the electric field i.e. < 150 V/ cm. Even though the flash occurred over a wide range of temperature and $pO_2$ the power density required for the flash transition lies within a narrow range (5- 25 mW $mm^{-3}$). This was also verified in dense GDC10 samples in Ar atmosphere ("Supplementary material", Figure S1). The said relation between atmosphere and flash temperature can be understood considering the higher electric conductivity of GDC10 in reducing environments. This can be easily observed in Figure 1(b), which points out that the power dissipation (and so also the conductivity) in Ar/$H_2$ surpasses the one in air during the FS incubation at given values of electric field and furnace temperature.

Extensive studies on transport properties and defects chemistry of GDC10 as a function of oxygen partial pressure are reported in the literature [35-36]. Here, the most important defects equilibria can be written as (Kröger-Vink notation):

$$O_O^X \leftrightarrow \frac{1}{2}O_2 + V_O^{\cdot\cdot} + 2e' \qquad \text{Eq. 2}$$

and

$$O_O^X + 2h^{\cdot} \leftrightarrow \frac{1}{2}O_2 + V_O^{\cdot\cdot}. \qquad \text{Eq. 3}$$

When ceria is reduced, it generates oxygen vacancies and electrons to maintain the charge neutrality. Part of these extra electrons are located on the cations

$$Ce_{Ce}^X + e' \leftrightarrow Ce_{Ce}' \qquad \text{Eq. 4}$$

which reduce their oxidation state form 4+ to 3+. Since $V_O^{\cdot\cdot}$ concentration is pinned by the loading of the substitution element (Gd), a reduction in $pO_2$ mainly results in an increase of electrons concentration and $Ce^{3+}$ species, enhancing the electronic *n-type* conductivity. The opposite behavior is expected in the case of *p-type* semiconductors, where conductivity decreases in reducing environments (Eq. 3) [37]. Therefore, the electrical conductivity enhancement at low $pO_2$ observed during FS incubation (Figure 1(b) and Figure S1) appears consistent with the activation of electronic *n-type* conductivity. We can also point out that the specimens flashed in Ar change their original pale yellow color to dark blue ("Supplementary Material", Figure S1 (d, e)). It is well-known that different stoichiometries in ceria-based materials account for different coloration, where blackening is related to a severe reduction of Ce ions from the 4+ to the 3+ state [38]. So, a partial reduction of the oxide is the origin of the electronic contribution to the conduction mechanism.

The above results raise the following question: "Is the influence of the n-type conductivity on flash, seen in the reducing atmosphere, also apply to flash experiments in air?" From the scientific literature this should not be so since the electronic conductivity is negligible in ceria at $pO_2 > 10^{-5}$ atm [39]. However, in FS experiments the sample is subjected to a DC bias of several tens or hundreds Volts, developing high local electric fields at the inter-particle contacts, that might affect the defect chemistry and activate new conduction mechanisms [40]. To answer this open question flash experiments were carried out on a hot plate in ambient air atmosphere to check the presence

of chromatic alterations associated to a partial reduction under the effect of electric loading (the so-called electrochemical blackening) [41].

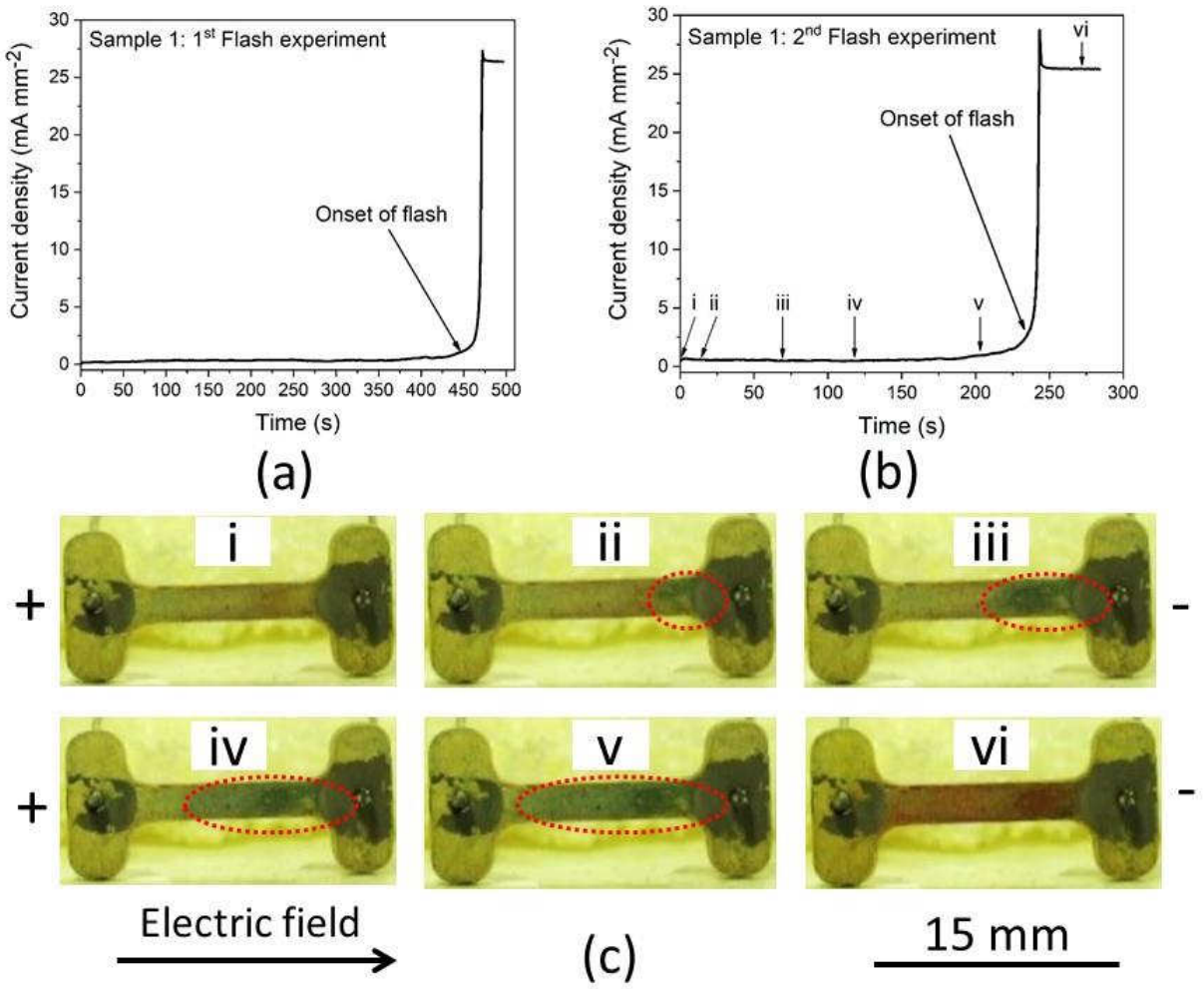


Figure 2. Chromatic alteration in the dense polycrystal GDC samples during the FS incubation in air (280°C, 150 V $cm^{-1}$, 25 mA $mm^{-2}$). (a) current density as a function of real time during the first flash experiment (b) current density as a function of real time during the second (repeated on the same specimen by reversing the electrode polarity) flash experiment (c) optical images of the samples during different stages of second flash experiment on the same sample revealing generation and propagation of the blackening from the negative to the positive electrode

During the incubation period of the flash experiment on the dense GDC polycrystal samples, a visible chromatic alteration develops in the early stage of the FS incubation from the negative electrode (cathode) and propagates towards the positive one (anode). Repeating the FS experiment on the same sample but with a reversed polarity. We can clearly observe that the blackening always starts at the cathode and propagates towards the anode. The chromatic alteration appears faint in the first experiment ("Supplementary material" Video) and more visible in the second run on the same sample (Figure 2 and "Supplementary material" Video S1). This is attributed to the fact that the

electric loading under DC bias forces an accumulation of oxygen vacancies in the cathodic region (-) where their charge is balanced by electrons injected from the metal electrode [38]:

$$\delta\, V_O^{\cdot\cdot} + CeO_2 + 2\delta\, e' \;\rightarrow\; CeO_{2-\delta} + \delta\, O^x \qquad . \qquad \text{Eq. 5}$$

Therefore, the material starts to be partially reduced from the cathode. The partially reduced region becomes electronically conductive; thus allowing the reduction reaction (taking place at the interface where electronic current is converted to ionic) to propagate through the sample. More interestingly, the incubation time for FS (i.e., the time needed to initiate the flash) in the repeated experiment (2nd time) is lowered by about 50% when compared to the first experiment. This suggests that, after the flash, the specimen retains a non-stoichiometric and free electrons-enriched state. In other words, there is a sort of "memory" of the previous flash process. This might be useful in the next future to tailor the electronic properties of both semiconducting and insulating oxides.

Electrochemical blackening suggests a change in the material stoichiometry due to the applied electric field, thus leading to the formation of electronic defects beyond the simple effect of temperature and molecular oxygen activity. The electronic conductivity is enhanced in the partially reduced state (Eq. 2) and, therefore, the current flow rises abruptly when the blackened region propagates to most of the gage length. The partial reduction of the oxide can be therefore considered a co-triggering mechanisms for FS in GDC, along with Joule heating.

To prove that (i) blackening is related to a partial reduction and (ii) this can be partially retained after the flash, XPS analysis were carried out on GDC10 before and after FS (here we are referring to the flash experiment in Figure 2).

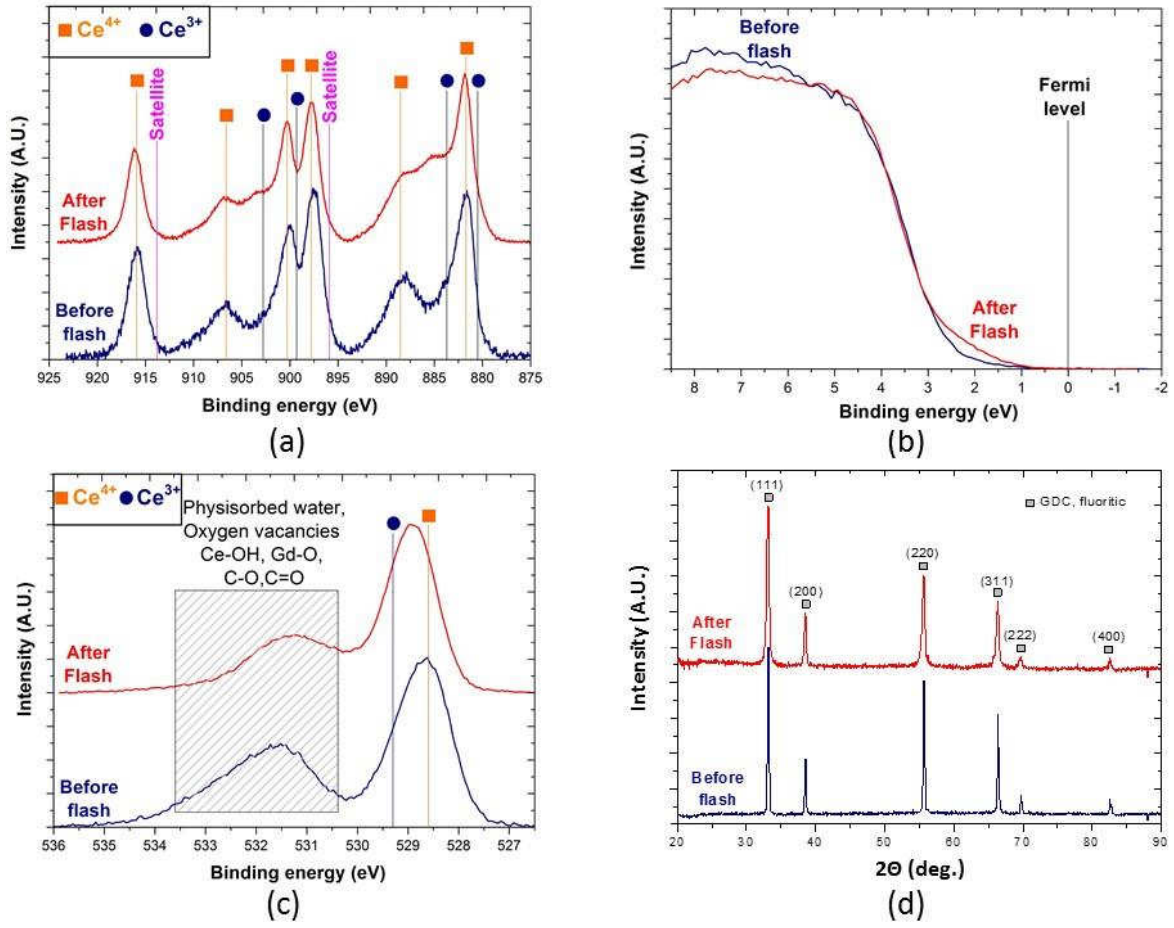

Figure 3. Comparison between GDC10 samples before and after flash in air: (a) Ce 3d; (b) valance band edge; and (c) O 1s XPS spectra (note that the signal at 531-533 eV is mainly related to surface impurities). The XRD patterns (d) are reported, as well.

Figure 3(a) shows the Ce 3d XPS spectrum before and after FS in air. The relative intensity of the spectral line associated with $Ce^{3+}$ increases after FS. This might be not very evident due to the presence of multiple peaks and the complex nature of the Ce XPS spectrum. However, if we focus our attention on the $Ce^{3+}$ lines at 884 and 903 eV, then we can conclude that their relative intensity rises after FS. A deconvolution (Supplementary material", Figure S2 and S3) of the spectra allows to point out a modification of the ratio between the intensities of the $Ce^{3+}$ and $Ce^{4+}$ components, the $Ce^{3+}/(Ce^{4+}+Ce^{3+})$ ratio passing from 0.26 (before flash) to 0.34 (after flash). This indicates that the sample is indeed reduced during the flash process. The results are also confirmed by a shift in the maximum XPS O 1s signal, which moves toward higher energies after FS (Figure 3 (c)). Such shift is consistent with a partial reduction of the oxide [32-33].

The crystalline structure of the flashed specimen was also investigated by XRD to verify that the reduction process did not cause the development of new phases [42]. The results point out that the sample fully retained its initial cubic fluorite structure (Figure 3 (d)), the reduced cations being therefore accommodated in solid solution in the parent fluorite phase. Thus, the crystallographic and electronic defects formation upon FS is strong enough to change the electric properties but it is not sufficient to induce any permanent structural alteration. In other words, when we focus our attention on FS mechanisms it is not necessary to seek huge effects involving a structural rearrangement of the material: in some cases faint effects of the field on the electronic structure are sufficient to change the electrical properties and conductivity.

Figure 3 (b) shows the XPS spectra of the valance band edge region before and after FS. We can observe that FS cause a small shift of the valance band edge at higher energy, thus resulting closer to the Fermi level. This suggests that FS might be responsible for a reduction of the band gap and due to the formation of donor levels connected to the oxygen vacancies created upon FS.

Finally, diffuse reflectance spectroscopy (DRS) measurements were carried out to verify the band gap energy ($E_g$) change by FS [34]. Figure 4(a) shows that the reflectance after FS is drastically reduced, pointing out the activation of new absorption mechanisms. This suggests an enhanced absorption of the flashed sample at low energy, that may be due to donor defects in the band gap region. Moreover, FS appears responsible for a decrease of the band gap, about 0.1 eV, as observed by drawing the tangent to the inflection point of the Kubelka-Munk plot (Figure 4(b)). It is worth mentioning that the results were obtained after the flash at room temperature. Schmerbauch et. al. studied the evolution of defects during flash sintering of ZnO by macro photoluminescence, shown that the defects are often modified during the flash state[43]. Therefore, a quantification of the $E_g$ change in the flash state remains an open question to be answered in the next future. However, our results clearly reveal that: (i) the electronic properties of GDC10 are modified upon FS and (ii) these alterations are partially retained after the flash. The introduction of defects by FS could be useful to develop new out-of-equilibrium materials.

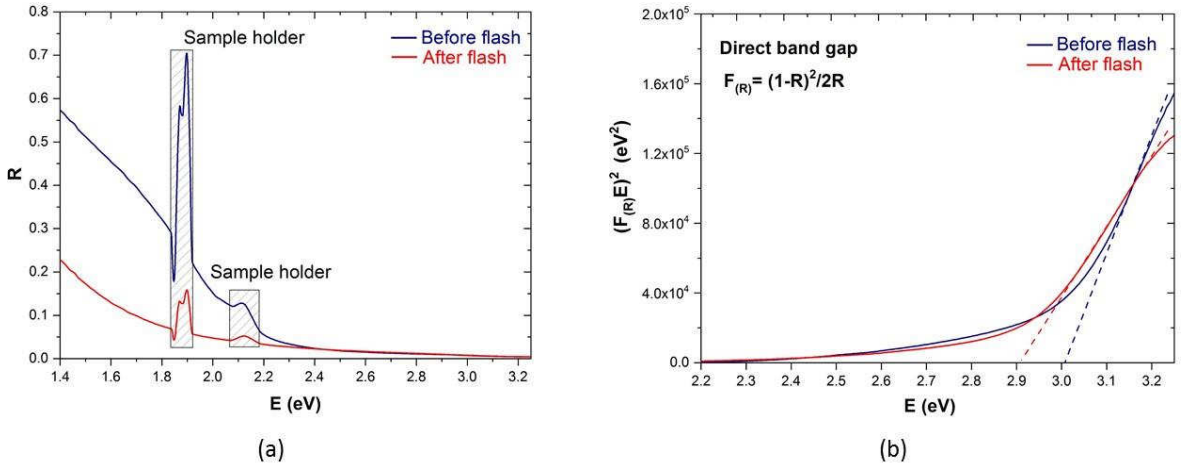


Figure 4. (a) diffuse reflectance (R); and (b) $(F_{(R)}E)^2$ vs. photon energy (E) plot for the determination of optical band gap of GDC10 before and after flash sintering.

In summary, the application of a DC electric field changes the electronic properties of GDC10 by moving the reduction front from cathode to anode electrode. The moving reduction front often heterogeneous at the microscopic scale while optically homogeneous at the macroscopic scale [44In particular, it activates *n-type* electronic conductivity which is associated to an electrochemical reduction process. Which causes growth of a microscopic filament as in memristive switching [45]. Such phenomenon appears to play a key role in the activation of FS. Visible chromatic alterations are observed during the process and are related to a change in the band gap of the specimen. The alteration of electronic structure is partially retained after FS as confirmed by XPS and DRS.

# Acknowledgements

This work is financially supported by the German Research Foundation (DFG) within the Priority Program on “Fields Matter” SPP 1959 [BR 3418/1-1]. R. Raj gratefully acknowledges support for this work from the Office of Naval Research under Grant No. N00014-18-1-2270. V.M: Sglavo and M. Biesuz kindly acknowledge support from the Italian Ministry of University and Research (MIUR) within the programs PRIN2017 - “DIRECTBIOPOWER” and Departments of Excellence 2018-2022 (DII-UNITN).

Mr. Giovanni Kiniger is warmly acknowledged for the collaboration.

# References


[1] M. Cologna, B. Rashkova, R. Raj, J Am Ceram Soc. 93 (11) (2010) 3556-3559.

[2] C. E. J. Dancer, Materials. Res. Express 3 (10) (2016) 102001.

[3] M. Yu, S. Grasso, R. Mckinnon, T. Saunders, M. J. Reece, *Adv*. *Appl*. *Ceram* 116 (2016) 24-60

[4] M.Z. Becker, N. Shomrat, Y. Tsur. Adv. Mater., 30 (2018) e1706369

[5] M. Biesuz, V. M. Sglavo, J Eur Ceram Soc. 39 (2019) 115-143

[6] R. Raj J. Am. Ceram. Soc., 99 (2016), pp. 3226-3232

[7] M. Biesuz, P. Luchi, A. Quaranta, A. Martucci, V. M. Sglavo, J EUR CERAM SOC., 37(9) (2017), 3125-3130.

[8] D. Yadav, & R. Raj, J. Am. Ceram. Soc., 100(12) (2017), 5374-5378.

[9] H. Yoshida, Y. Sakka, T. Yamamoto, J.M. Lebrun, R. Raj, J. Eur. Ceram. Soc., 34 (2014), pp. 991-1000

[10] X. Hao, Y. Liu, Z. Wang, J. Qiao, K. Sun, J. Power Sources, 210 (2012), pp. 86-91

[11] M. Biesuz, V.M. Sglavo, J. Eur. Ceram. Soc., 36 (2016), pp. 2535-2542

[12] D. Yadav, R. Raj, J. Am. Ceram. Soc., 100 (2017), pp. 5374-5378

[13] T. P. Mishra, V. Avila, R.R.I. Neto, M. Bram, O. Guillon, R. Raj, Scr. Mater., 170(2019), pp.81-84.

[14] M. Jongmanns M, R. Raj, D. Wolf, New J Phys. 20 (9) (2018) 093013.

[15] R.I. Todd, E. Zapata-Solvas, R.S. Bonilla, T. Sneddon, P.R. Wilshaw, J. Eur. Ceram. Soc., 35 (2015), pp. 1865-1877

[16] Y. Zhang, J.I. Jung, J. Luo, Acta Mater., 94 (2015), pp. 87-100

[17] W. Ji, B. Parker, S. Falco, J.Y. Zhang, Z.Y. Fu, R.I. Todd, J. Eur. Ceram. Soc., 37 (2017), pp. 2547-2551

[18] K. S. Naik, V. M. Sglavo, R. Raj, J. Eur. Ceram. Soc., 34 (2014), pp. 4063-4067

[19] R. Chaim, Materials, 10 (2017), p. 179

[20] J. Narayan, Scr. Mater., 68 (2013), p. 785

[21] M. Jongmanns, D. E. Wolf, J. Am. Ceram. Soc., 00(2019), pp. 1-8

[22] J. M. Lebrun,, & R. Raj, J. Am. Ceram. Soc., 97(8) (2014), pp. 2427-2430

[23] L. Spiridigliozzi, M. Biesuz, G. Dell'Agli, E. Di Bartolomeo, F. Zurlo, V.M. Sglavo, J. Mater. Sci., 52 (2017), pp. 7479-7488

[24] L. Spiridigliozzi, L. Pinter, M. Biesuz, G. Dell'Agli, G. Accardo, V.M. Sglavo, Materials (Basel), 12 (8) (2019)

[25] T. Jiang, Z. Wang, J. Zhang, X. Hao, D. Rooney, Y. Liu, W. Sun, J. Qiao, K. Sun J. Am. Ceram. Soc., 98 (2015), pp. 1717-1723

[26] S.K. Jha, H. Charalambous, H. Wang, X.L. Phuah, C. Mead, J. Okasinski, H. Wang, T. Tsakalakos, Ceram. Int. 44 (13) (2018) 15362–15369

[27] Y.Y. Zhang, J. Luo, Scr. Mater., 106 (2015), pp. 26-29

[28] D. Yadav, R. Raj, Scr. Mater. 134 (2017) 123-127

[29] M. Biesuz, L. Pinter, T. Saunders, M. Reece, J. Binner, V.M. Sglavo, S. Grasso, Materials, 11 (2018), p. 1214

[30] S. Jo, R. Raj, Scr. Mater., 174 (2020), pp.29-32

[31] M. Cologna, J. Francis, R. Raj, J Eur Ceram Soc. 31 (15) (2011) 2827-2837

[32] M. Romeo, K. Bak, J. El Fallah, F. Le Normand, L. Hilaire, Surf. Interf. Anal., 20 (1993), pp. 508 – 512

[33] L. H. Chan and J. Yuhara, J. Chem. Phys., 143 (2015), pp. 074708/1 – 074708/8

[34] R. López and R. Gómez, J. Sol–Gel Sci. Technol., 61(2012), pp. 1–7

[35] W. Lai, S.M. Haile, J. Am. Ceram. Soc. 88(2005), pp. 2979–2997

[36] S. Wang, T. Kobayashi, M. Dokiya, T. Hashimoto, *J. Electrochem. Soc.*, 147(10)(2000), pp.3606-3609.

[37] Y.-M. Chiang, D.P. Birnie, W.D. Kingery, S. Newcomb, Physical Ceramics: Principles for Ceramic Science and Engineering, Wiley, Chichester, 1997.

[38] M. Mogensen, N.M. Sammes, G.A. Tompsett, Solid State Ionics, 129(1-4) (2000), pp.63-94.

[39] H. Yahiro, Y. Eguchi, K. Eguchi, H. Arai, J. Appl. Electrochemistry 18 (1988) 527–531.

[40] X. Vendrell,A. R. West, J. Am. Ceram. Soc. 2019, IN PRESS.

[41] J. Janek, C. Korte, Solid State Ionics, 116(3-4) (1999), pp.181-195.

[42] V. Esposito, et al., Acta Mater., 61 (2013), p. 6290

[43] C. Schmerbauch, J. Gonzalez-Julian, R. Röder, C. Ronning, O. Guillon, Journal of the American Ceramic Society 97 (2014) 1728–1735

[44] R. Kirchheim, Acta Materialia 175 (2019) 361–375

[45] D.H. Kwon, S. Lee, C.S. Kang, Y.S. Choi, S.J. Kang, H.L. Cho, W. Sohn, J. Jo, S.Y. Lee, K.H. Oh, T.W. Noh, R.A.D. Souza, M. Martin, M. Kim, Advanced Materials 31 (2019) 1901322